

MBE-Grown CdTe Layers on GaAs with In-assisted Thermal Deoxidation

OZAN ARİ ^{1,3,4,5} ELIF BILGILISOY,^{1,3} ELIF OZCERI,^{1,2,3}
and YUSUF SELAMET^{1,3}

1.—Department of Physics, Izmir Institute of Technology, Izmir, Turkey. 2.—Department of Material Science and Engineering, Izmir Institute of Technology, Izmir, Turkey. 3.—Infrared and Micro-Electronic Material Research Laboratory (IRMAM), Izmir Institute of Technology, Izmir, Turkey. 4.—e-mail: ozanari@gmail.com. 5.—e-mail: ozanari@iyte.edu.tr

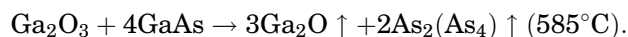
Molecular beam epitaxy (MBE) growth of thin ($\sim 2 \mu\text{m}$) CdTe layers characterized by high crystal quality and low defect density on lattice mismatched substrates, such as GaAs and Si, has thus far been difficult to achieve. In this work, we report the effects of *in situ* thermal deoxidation under In and As₄ overpressure prior to the CdTe growth on epitaxially grown GaAs(211)B wafers, aiming to enhance CdTe crystal quality. Thermally deoxidized GaAs samples were analyzed using *in situ* reflection high energy electron diffraction, along with *ex situ* x-ray photo-electron spectroscopy (XPS) and atomic force microscopy. MBE-grown CdTe layers were characterized using x-ray diffraction (XRD) and Everson-type wet chemical defect decoration etching. We found that In-assisted desorption allowed for easier surface preparation and resulted in a smoother surface compared to As-assisted surface preparation. By applying In-assisted thermal deoxidation to GaAs substrates prior to the CdTe growth, we have obtained single crystal CdTe films with a CdTe(422) XRD rocking curve with a full-width half-maximum value of 130.8 arc-s and etch pit density of $4 \times 10^6 \text{ cm}^{-2}$ for 2.54 μm thickness. We confirmed, by XPS analysis, no In contamination on the thermally deoxidized surface.

Key words: MBE, GaAs deoxidation, CdTe growth, XPS, RHEED, XRD

INTRODUCTION

High-quality epitaxial CdTe layers are desirable as a buffer to HgCdTe (MCT) growth on alternative substrates (Si, GaAs, and GaSb), and have potential application in the development of photo-detectors and solar cells. Authors of most extant studies report producing highly crystalline CdTe epitaxial layers with low defect density on Si, GaAs, and GaSb substrates, albeit for thicknesses exceeding 7 μm .^{1,2} Growth of thin CdTe layers (2–4 μm) with sufficient crystal quality is important for reducing production time/cost of MCT infrared detectors and photovoltaic solar cells grown using the molecular beam epitaxy (MBE) technique. However, the crystal quality and defect density of the CdTe layers are

greatly affected by substrate preparation and growth conditions. The thermal deoxidation process plays a crucial role in MBE growth of CdTe layers. Thermal desorption of the most As-oxide and Ga-oxide species from the GaAs surface—which is an integral part of substrate preparation—requires temperatures of up to 400°C.^{3,4} However, the non-volatile Ga₂O₃ molecule is stable at temperatures of up to 1000°C.^{4,5} Fortunately, Ga₂O₃ desorption from the GaAs surface can be accomplished with the help of GaAs molecules at the surface temperature of 585°C, through the following reaction⁶:



Furthermore, the deoxidation duration of Ga₂O₃ at 585°C depends on the oxide thickness and oxide composition of the GaAs substrate. However, thermal desorption is hindered by the fact that Ga

(Received November 17, 2015; accepted February 19, 2016;
published online March 8, 2016)

consumption during Ga₂O₃ desorption creates pits 50–200 nm in size and 5–40 nm in depth on the GaAs surface, which may reduce the interface and compromise the overall quality of the consecutively grown CdTe layer.^{4,5} Successful utilization of In-assisted thermal deoxidation⁷ at lower temperatures, aiming to prevent further surface damage during thermal deoxidation of GaAs substrates, has been reported. The authors noted that, as In atoms react to non-volatile Ga₂O₃ molecules more effectively compared to the Ga atoms, this results in an atomically smooth surface, achieved through the following reaction⁷:



In this work, we investigated the effects of In-assisted thermal deoxidation on GaAs substrate surface morphology and compared these outcomes with those achieved by As-assisted deoxidation. As a part of this work, we also characterized MBE-grown CdTe epitaxial layers in order to understand the deoxidation process effects. In addition, we studied defect incursions from the GaAs–CdTe interface to the CdTe surface.

EXPERIMENTAL

Thermal deoxidation and CdTe growth were performed in a Veeco GEN20MZ MBE system using 20 × 20 mm² GaAs(211)B epi-ready substrates. Thermal deoxidation was carried out with a Veeco Mark V 500 As (7 N) valved cracker and atomic source In (7 N), whereas CdTe growth was performed with Veeco Mark V 200 CdTe (7 N) and Te (7 N) valved crackers. Thermal deoxidation and growth was monitored *in situ* through reflection high-energy electron diffraction (RHEED), which yielded data pertaining to surface crystal quality. In addition, a calibrated pyrometer was used for temperature measurement.

GaAs substrates were heated from room temperature to 585°C and were kept at this temperature for ~5 min under As₄ flux with 2.5 × 10⁻⁶ Torr beam equivalent pressure (BEP), which was initiated at the surface temperature of 300°C for the As₄-assisted deoxidation procedure. In-assisted deoxidation was carried out in three steps, commencing with (1) increasing the GaAs substrate temperature to 530°C without any flux, followed by (2) supplying In flux with 4.5 × 10⁻⁸ Torr BEP to the surface for 3 min, and culminating in (3) increasing the temperature to 550°C, which was maintained for 3 min for In-related material (InAs, InO₂) desorption.⁷ Next, GaAs substrates were cooled under As₄ flux with 2.5 × 10⁻⁶ Torr BEP to ensure B polarity of the GaAs substrate in both As- and In-assisted deoxidation processes. CdTe growth was initiated with nucleation at ~210°C, before being annealed at ~385°C. The thickness of the nucleation layers was ~150 nm. The thick CdTe layer growth was performed at ~300°C. Three CdTe

layers were grown to 2.3–2.5 μm thickness, at the rate of ~1 μm/h. Additionally, *in situ* cycling annealing at 395°C was applied to one sample to improve the crystal quality and reduce the dislocation density.⁸

GaAs substrates were characterized using x-ray photo-electron spectroscopy (XPS), which yielded data pertaining to the surface chemical composition. XPS measurements were performed with an Al x-ray source and a SPECS Phoibos 150 Hemispherical Analyzer. Large area focus and 40 eV E-pass energy was chosen to achieve the best signal-to-noise ratio in the XPS spectra. The surface morphology of GaAs substrates was characterized using atomic force microscopy (AFM). The crystal quality of the CdTe layers was determined with high-resolution four-crystal x-ray diffraction (XRD). Defect propagation from the GaAs–CdTe interface to the CdTe surface was determined via the wet chemical defect decoration etching method. More specifically, 15 s (1HF:4HNO₃:25H₂O) Everson-type⁹ etching was applied to the CdTe layers, allowing the etch pit density (EPD) to be calculated using scanning electron microscopy (SEM) images.

RESULTS AND DISCUSSION

To analyze the surface crystal quality evolution of GaAs substrates, RHEED images and spot intensities were recorded from the [0–11] azimuth, in order to ensure consistency across different deoxidation processes during deoxidation of the GaAs substrates.¹⁰ Figure 1 shows the RHEED images of the epi-ready surface and thermal deoxidation effects under As₄ and In overpressures. Bright and streaky spots became discernible after both As₄- and In-assisted deoxidation processes. However, RHEED spots were brighter and streakier following In-assisted thermal deoxidation. Figure 2 shows the temperature profiles and intensity evaluation of a RHEED spot, which is marked in Fig. 1 with a yellow circle. We noted the emergence of one smooth RHEED spot with an intensity increase at ~350°C, which was saturated after 5 min at 585°C during As₄-assisted deoxidation. RHEED spot intensity saturation suggested the completion of thermal deoxidation, which we established to be about 5 min at 585°C for an optimal deoxidation duration with As₄ overpressure. In addition, we observed two abrupt intensity changes during In-assisted thermal deoxidation, the first of which occurred ~1.5 min after the In shutter was opened at 530°C. The second abrupt RHEED spot intensity change took place while heating to 550°C for In-related desorption from the GaAs surface. RHEED spot intensity continued to increase for a while after As₄ shutter was opened during the GaAs substrate cool-down period. We thus surmise that In molecules reacted with Ga₂O₃ and desorbed from the GaAs surface, which first caused an abrupt change in RHEED spot intensity. We also postulate that

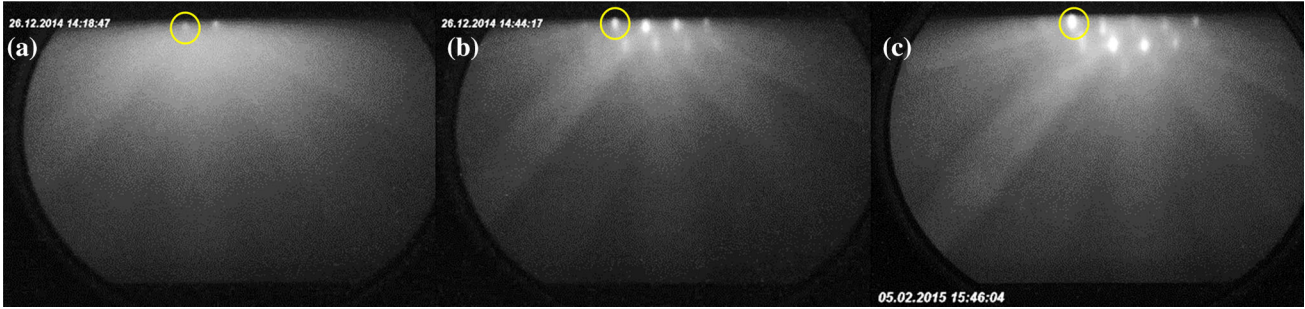


Fig. 1. *In situ* RHEED patterns of the GaAs(211)B surface, taken from the [0–11] azimuth; (a) epiready, (b) thermally deoxidized under As overpressure, (c) thermally deoxidized under In overpressure.

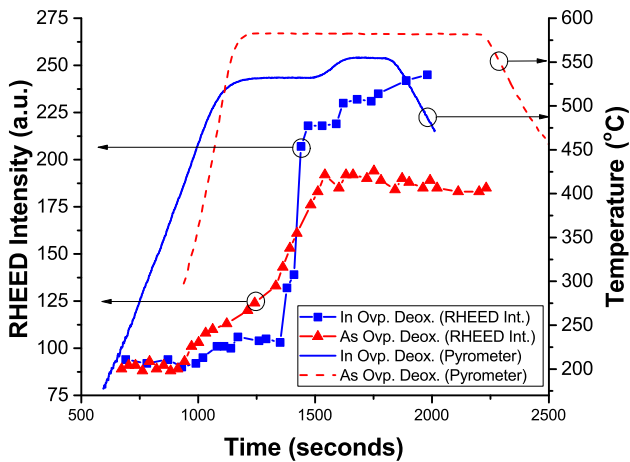


Fig. 2. RHEED spot intensity and surface temperature (Pyrometer) change during deoxidation. Blue (red) lines corresponds to the In-(As-) assisted deoxidation (Color figure online).

InO_2 and InAs might remain on the surface for a further 3 min following the exposure of the GaAs surface to In overpressure. In such a scenario, we posit that the second abrupt change in intensity stems from desorption of those In-related materials from the surface as the surface temperature increases to 550°C . It should be noted that the ratio of intensity change with respect to that noted at the beginning of deoxidation was ~ 1.33 higher for In-assisted relative to As_4 -assisted desorption. We propose that the appearance of brighter RHEED spots and streakier RHEED patterns after In-assisted deoxidation is indicative of an atomically smoother surface compared to that achieved by As_4 -assisted deoxidation.

For further characterization of surface states, deoxidized samples were removed from the MBE chamber and transferred to the XPS chamber along with as-received epiready wafers. As_2O_5 , As_2O_3 , Ga_2O , and Ga_2O_3 oxide species were found in the as-received epiready GaAs wafer surfaces. Figure 3 shows As 3d and Ga 3d spectra of samples thermally deoxidized under In and As_4 overpressures. The As_2O_5 state was not present for samples thermally deoxidized with either method. However, a slight

contribution from the As_2O_3 states to the As 3d spectra was noted in both cases. Similarly, the Ga_2O_3 state was not detected, while the Ga_2O states were observed in the Ga 3d spectra of samples subjected to both In and As_4 overpressure deoxidation. In 4d-related peaks were not observed, even though they were expected to emerge near the Ga 3d peaks in the Ga 3d XPS spectra of thermally deoxidized samples under In overpressure. We posit that the absence of As_2O_5 and Ga_2O_3 states in relevant XPS spectra suggests the completion of deoxidation processes in both cases. On the other hand, the presence of As_2O_3 and Ga_2O states in relevant XPS spectra is due to exposure to air during the transfer of the samples to the XPS chamber.

Surface morphologies of both thermally deoxidized and as-received epiready samples were characterized by AFM. AFM height images of thermally deoxidized samples under As_4 and In overpressures are given in Fig. 4. Figure 4a and b shows that thermal deoxidation under As_4 overpressure created surface features with larger dimensions compared to those obtained under In overpressure. To further characterize the surface pits, AFM images were adjusted to show only pits on the surface. These AFM images of thermally deoxidized samples under As_4 and In fluxes are presented in Fig. 4c and d, respectively. Figure 4c shows that thermal deoxidation under As_4 overpressure created large pits on the sample surface. Statistical analysis was performed on the AFM height images in order to obtain root-mean-square (RMS) roughness, peak-to-peak distance, skewness, and the surface pit population. The statistical analysis results are given in Table I. As can be seen from the data, RMS roughness and maximum peak-to-peak distance of the epiready wafer surface altered slightly after thermal deoxidation under In and As_4 fluxes. Skewness of the epiready surface changed from being a hill-dominant to a slightly pit-dominant surface. Pit number density on the sample surfaces was calculated from AFM images with particle analysis and discrete frequency analysis. Pit percentages were calculated in the range of 12 nm to the maximum detected pit size for each sample. Pit number density of pits

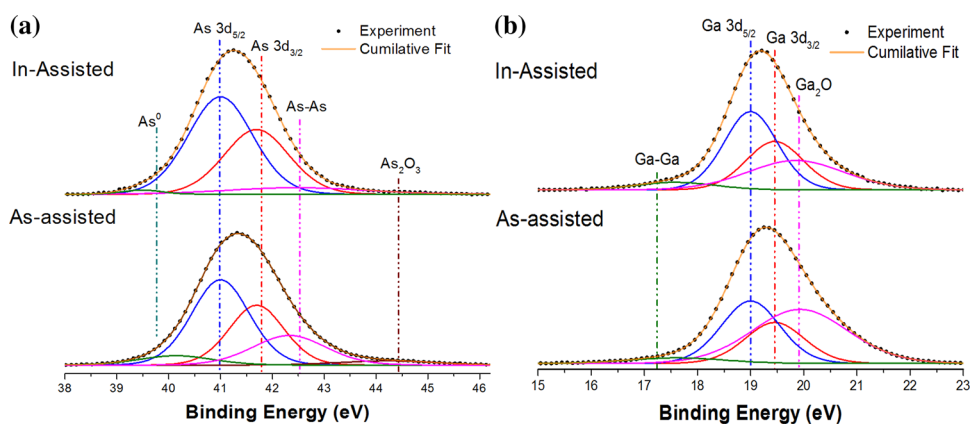


Fig. 3. (a) As 3d and (b) Ga 3d XPS spectra of thermally deoxidized GaAs samples under In and As₄ fluxes.

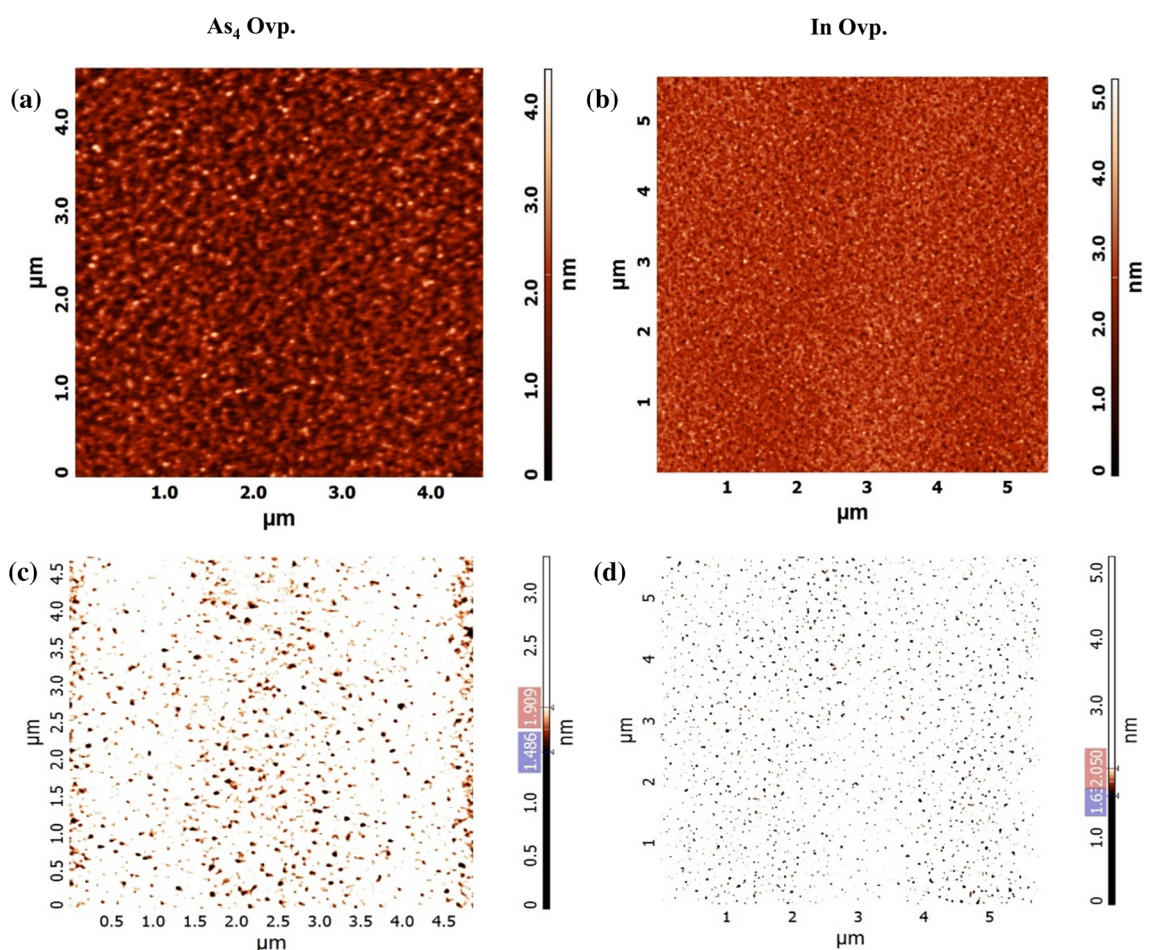


Fig. 4. AFM height images of the samples deoxidized under (a) As overpressure and (b) In overpressure. Contrast-adjusted AFM height images of the samples deoxidized under (c) As overpressure and (d) In overpressure.

larger than 25 nm on epitaxial GaAs surfaces increased by 14% and 2% for samples thermally deoxidized under As₄ and In, respectively. The occurrence of fewer pits on thermally deoxidized samples under In overpressure is in agreement with the RHEED results.

To demonstrate thermal deoxidation effects on MBE-grown epilayers, 2.34–2.54 μm CdTe layers were grown on thermally deoxidized GaAs substrates. Figure 5 provides the XRD rocking curve results from the CdTe(422) reflection with the [0–11] azimuth for CdTe layers grown on thermally

Table I. AFM measurement results of the epitaxially and thermally deoxidized GaAs samples under As and In overpressures

	Deox. time (s)	Deox. temp. (°C)	Peak to peak (nm)	Roughness (RMS) (nm)	Skewness	Percentages of the pits		Max. pit size (nm) ^a
						>35.7 nm (%) ^a	>50.5 nm (%) ^a	
Epitaxially	–	–	4.76	0.42	0.229	17	6	61.8
As as. deox.	315	585	5.12	0.35	−0.082	22	15	71.4
In as. deox.	210	530	5.61	0.45	−0.068	18	7	71.4

^aPit sizes were calculated with 0.05 nm accuracy.

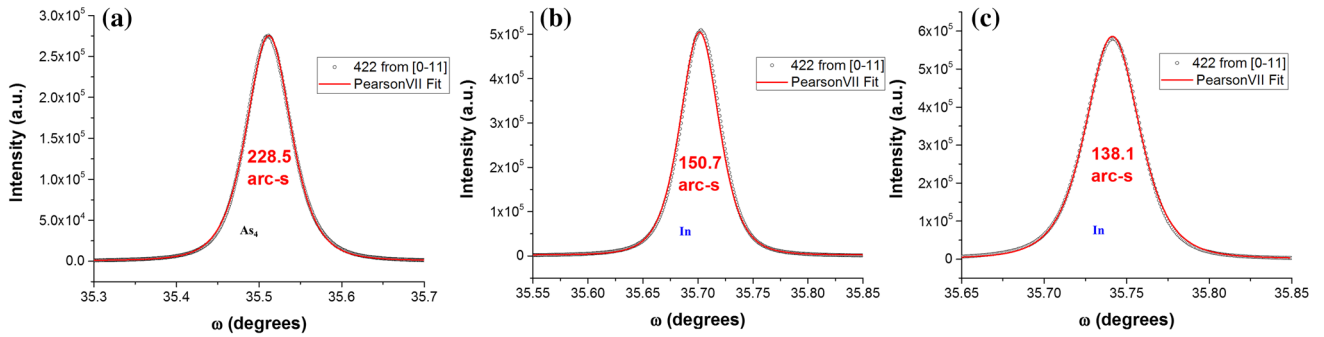


Fig. 5. Four crystal high-resolution XRD rocking curves of CdTe layers on thermally deoxidized layers under (a) As_4 overpressure, and (b) In overpressure. Additionally, a cyclic annealing procedure was applied for (c) after thermal deoxidation under In overpressure.

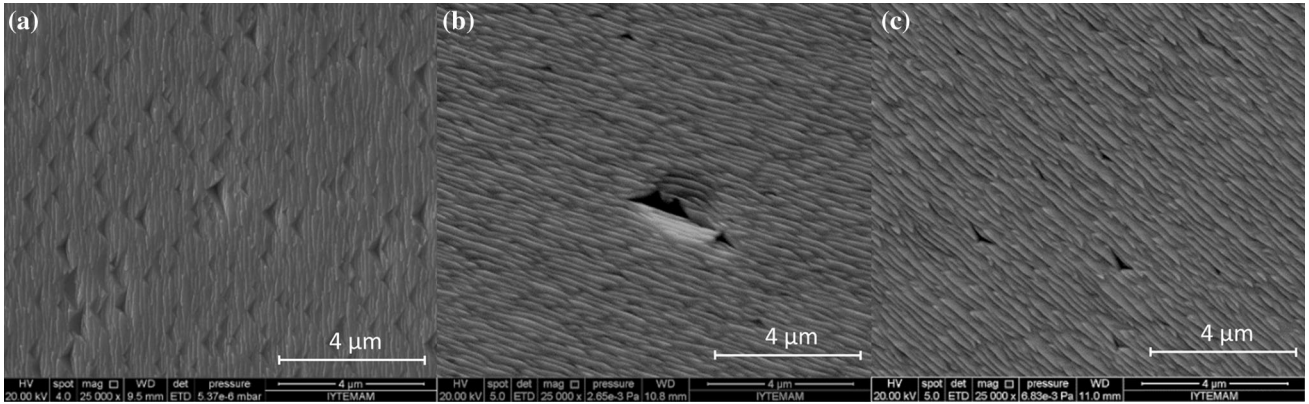


Fig. 6. Post-Everson etching SEM images of CdTe layers on thermally deoxidized layers under (a) As_4 overpressure, and (b) In overpressure. Additionally, a cyclic annealing procedure was applied for (c) after thermal deoxidation under In overpressure.

deoxidized GaAs substrates (Fig. 5a) under As_4 overpressure, and (Fig. 5b) under In overpressure, with (Fig. 5c) showing the results after a cyclic annealing procedure was applied in order to achieve the best crystal quality for CdTe layers. FWHM values pertaining to the CdTe samples grown on thermally deoxidized surfaces under In overpressure were 78–98 arc-s lower compared to those obtained in the case of As-assisted thermal deoxidation. However, it should be noted that a small decrease in FWHM values with increasing layer thickness is expected.¹ Nonetheless, the observed

78–98 arc-s difference in the FWHM values for 2.34–2.54 μm thick layers is not solely related to the thickness difference of the CdTe layers. An XRD rocking curve FWHM value of 138.1 arc-s for the 2.54- μm layer was obtained using cyclic annealing during CdTe growth. This value is in good agreement with the best reported FWHM values for this thickness.¹

To further characterize the crystal quality of CdTe layers, Everson-type etching was applied to the samples. Figure 6 shows the post-Everson etching SEM images of CdTe layers grown on thermally

deoxidized GaAs substrates (Fig. 6a) under As₄ overpressure, and (Fig. 6b) In overpressure, with Fig. 6c depicting the results obtained after cyclic annealing was applied during CdTe growth of the sample. EPD were calculated from SEM images of the samples in cases Fig. 6a, b, and c as $1.1 \times 10^8 \text{ cm}^{-2}$, $1.1 \times 10^7 \text{ cm}^{-2}$, and $4 \times 10^6 \text{ cm}^{-2}$, respectively. Thermal deoxidation of GaAs samples under In overpressure caused a decrease in defect density of CdTe layers grown under the same conditions (equivalent to about one order of magnitude). Cyclic annealing resulted in a further decrease in the EPD value (by nearly two orders of magnitude) compared to that pertaining to the CdTe layer grown on GaAs thermally deoxidized sample under As overpressure.

CONCLUSIONS

In-assisted and commonly used As₄-assisted thermal deoxidation procedures were applied to GaAs(211)B epi-ready substrates and were subsequently characterized. RHEED analysis showed that In-assisted deoxidation created streakier and ~1.33 times brighter spots compared to those obtained by As₄-assisted deoxidation. Desorption of non-volatile Ga₂O₃ molecules from GaAs substrates after thermal deoxidation was confirmed for both In- and As₄-assisted deoxidation procedures. Additionally, no In-related states were observed in the XPS spectra of the GaAs samples. RHEED results were confirmed by subsequent AFM measurements. Pit number density in AFM images of thermally deoxidized sample under In overpressure remained almost the same as those pertaining to the epi-ready GaAs wafer. On the other hand, a 23% increase in pit number density was observed after As₄-assisted deoxidation of GaAs substrates. The crystal quality of the CdTe layers grown on thermally deoxidized GaAs substrates under In overpressure was superior to the CdTe layers grown on thermally deoxidized GaAs substrates under As₄ overpressure. An EPD value of $4 \times 10^6 \text{ cm}^{-2}$ for 2.54 μm was

obtained by applying cyclic annealing during CdTe layer growth after In-assisted deoxidation of the GaAs substrates. To our knowledge, this EPD value is the lowest reported for 2.54-μm-thick MBE-grown CdTe. These results indicate that In-assisted deoxidation of GaAs substrates creates a smooth and nearly Ga-related pit-free surface. Thus, we have demonstrated that CdTe layers with improved crystal quality and lower defect density for thin ~2.5-μm layers are obtainable for CdTe growth on thermally deoxidized GaAs wafers under In overpressure.

ACKNOWLEDGEMENTS

We are grateful to Dr. Orhan Öztürk from Izmir Institute of Technology for XRD measurements. We are also acknowledge the usage of XPS system at AQUIREC Laboratories at Izmir Institute of Technology.

REFERENCES

1. L. He, X. Fu, Q. Wei, W. Wang, L. Chen, Y. Wu, X. Hu, J. Yang, Q. Zhang, R. Ding, X. Chen, and W. Lu, *J. Electron. Mater.* 37, 1189 (2008).
2. R.N. Jacobs, L.A. Almeida, J. Markunas, J. Pellegrino, M. Groenert, M. Jaime-Vasquez, N. Mahadik, C. Andrews, S.B. Qadri, T. Lee, and M. Kim, *J. Electron. Mater.* 37, 1480 (2008).
3. T. Van Buuren, M.K. Weilmeier, I. Athwal, K.M. Colbow, J.A. Mackenzie, P.C. Wong, and K.A.R. Mitchell, *Appl. Phys. Lett.* 59, 464 (1991).
4. A. Guillén-Cervantes, Z. Rivera-Alvarez, M. López-López, E. López-Luna, and I. Hernández-Calderón, *Thin Solid Films* 373, 159 (2000).
5. F. Bastiman, R. Hogg, M. Skolnick, A.G. Cullis, and M. Hopkinson, *J. Phys.: Conf. Ser.* 209, 012066 (2010).
6. A.S. Thorpe and S. Ingre, *Appl. Phys. Lett.* 50, 77 (1987).
7. L.H. Li, E.H. Linfield, R. Sharma, and A.G. Davies, *J. Appl. Phys. Lett.* 99, 2 (2011).
8. C.M. Lennon, L.A. Almeida, R.N. Jacobs, J.D. Benson, P.J. Smith, J.K. Markunas, J. Arias, and J. Pellegrino, *J. Electron. Mater.* 42, 3344 (2013).
9. W.J. Everson, C.K. Ard, J.L. Sepich, B.E. Dean, G.T. Neugebauer, and H.F. Schaake, *J. Electron. Mater.* 24, 505 (1995).
10. J.P.A. der Wagt, PhD thesis, Reflection High Energy Electron Diffraction During Molecular Beam Epitaxy. (Stanford University, 1994).